Eur Biophys J (2008) 37:1309–1316
DOI 10.1007/s00249-008-0337-5

ORIGINAL PAPER

New horizons of adenosinetriphosphate energetics arising from interaction with magnesium cofactor

Alexander A. Tulub · V. E. Stefanov

Received: 25 October 2007 / Accepted: 3 April 2008 / Published online: 8 May 2008

Abstract MD DFT:B3LYP (6-31G** basis set, $T = 310$ K) method is used to study interactions [singlet (S) and triplet (T) reaction paths] between adenosinetriphosphate, ATP^{4-}, and $[Mg(H_2O)_6]^{2+}$ in water environment, modeled with 78 water molecules. Computations reveal the appearance of low and high-energy states (stable, quasi-stable, and unstable), assigned to different spin symmetries. At the initial stage of interaction, ATP donates a part of its negative charge to the Mg complex making the Mg slightly charged. As a result, the original octahedral Mg complex loses two (S state) or four (T state) water molecules. Moving along S or T potential energy surfaces (PESs), $Mg(H_2O)_4$ or $Mg(H_2O)_2$ display different ways of complexation with ATP. S path favors the formation of a stable chelate with the O1–O2 fragment of ATP triphosphate tail, whereas T path favors producing a single-bonded complex with the O2. The latter, being unstable, undergoes a further conversion into a spin-separated complex, also unstable, and two metastable S complexes, which finally arise in two stable, low-energy and high-energy, chelates. The spin-separated complex experiences rapid decomposition resulting in the production of a highly reactive adenosinemonophosphate ion-radical •AMP, early observed in the CIDNP experiment (Tulub 2006). Biological consequences of the findings are discussed.

Keywords MD DFT · ATP · Mg complexes

A. A. Tulub (✉)
Department of Chemistry and Chemical Biology,
Harvard University, 12 Oxford Street,
Cambridge, MA 02138, USA
e-mail: atulub@yahoo.co.uk

A. A. Tulub · V. E. Stefanov
Department of Biophysics and Biochemistry,
Computational Modeling Group, Saint-Petersburg State
University, Universitetskaya Embankment 7/9,
Saint-Petersburg 199034, Russian Federation

Introduction

Without any exaggeration adenosinetriphosphate (ATP), (Fig. 1), can be considered as the most important and fascinating molecule in living nature, thanks to its ability to maintain the energy balance in living cells and initiate numerous biochemical reactions by releasing an imposing amount of energy, 7.3–10.9 kcal/mol, which is then regained via recycling, a repeated process that occurs 2,000–3,000 times a day (Stryer 2002; Audesirk and Audesirk 1999; Levy 1982; Nave and Nave 1985; Nelson and Cox 2004; Tuszynski and Dixon 2002). The energy is stored in the ATP triphosphate tail (TT), (Fig. 1), and its release, as widely accepted, results from the ATP hydrolysis, partial ($\Delta E = -7.3$ kcal/mol) or total ($\Delta E = -10.9$ kcal/mol) (Stryer 2002), accompanied by the production of adenosinediphosphate (ADP), or adenosinemonophosphate (AMP), respectively (Nelson and Cox 2004; Stryer 2002; Nelson 2004). In water containing environment, like living cells, ATP is quite stable. Its hydrolysis suggests overcoming a significant energy barrier of about 25 kcal/mol (Okimoto et al. 2001; Akola and Jones 2003; Grigorenko et al. 2006). The hydrolysis, conventionally considered as an ionic reaction (Okimoto et al. 2001; Akola and Jones 2003; Grigorenko et al. 2006), is slow and produces the ionic forms of ADP and AMP (Nave and Nave 1985; Nelson and Cox 2004). However, a significant number of polymerization reactions, accompanied by NTP→NDP or NTP→NMP [N = nucleosidetriphosphate; N = A (adenosine), C (cytidine), G

(guanosine), T (thymidine), U (uridine)] conversion, are highly rapid. They proceed in a picosecond–nanosecond interval (Tulub and Stefanov 2004) and according to the "living chain" polymerization mechanism (Odian 1991), which suggests the appearance of free radicals as intermediates (Korolev and Marchenko 2000; Tulub and Stefanov 2004; Tulub 2006). These reactions include tubulin assembly into microtubules (NTP = GTP) (Dustin 1984; Sept et al. 1999; Tulub and Stefanov 2004) and DNA/RNA single chain polymerization (Korolev and Marchenko 2000; Stefanov and Tulub 2007). In these reactions, the diphosphate and monophosphate products are not inert. They are strongly involved into spin transferring ion-radical reactions (Tulub and Stefanov 2004; Tulub 2006). The typical hydrolysis is unable to explain the production of free radicals (Korolev and Marchenko 2000). The reason is that ATP, and NTP in general, has been considered in the context of the lowest molecular energetics without including the high-energy states, differing in spin and showing minima in separated regions around O1–O3, (Fig. 1).

From the very beginning of ATP studies in vitro and in vivo, it has been repeatedly proved that Mg^{2+} cations (Mg cofactor) are permanent partners in the ATP cleavage (Ochoa 1964; Boyer 1997; Walker 1997; Shien et al. 1999; Stryer 2002). However, the mechanism of this process is still elusive (Tulub 2006). For instance, it is unclear why Mg and not other cation, say Ca, Zn, Fe or Mn, are required. This barely be explained by the cation size because the distances between the O1, O2, and O3 atoms, the major targets of the cation attack on ATP, are quite remarkable, ~4 Å, and flexible to adjust to the size of the counterpart cation or its complex (Stryer 2002; Nelson 2004).

It was proved that interaction between Mg^{2+} and ATP mostly ends up in chelating the O1–O2 fragment and less commonly in the O2–O3 one (Audesirk and Audesirk 1999; Levy 1982; Nave and Nave 1985; Stryer 2002; Williams 2000), Fig. 1, and up to the moment this widely known fact has no physical explanation (Nelson and Cox 2004). A number of authors consider chelation responsible for

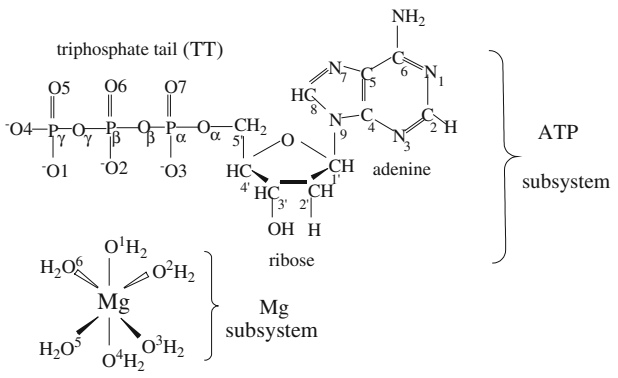

Fig. 1 Structure of the ATP and Mg subsystems

decreasing the activation barrier of TT cleavage against that of typical hydrolysis without Mg^{2+} (Akola and Jones 2003; Grigorenko et al. 2006). The decrease, however, is not high, ~5 kcal/mol, and unlikely to account for the rapid free radical production, recently detected experimentally with the chemically induced dynamic nuclear polarization (CIDNP) technique (Tulub 2006; Stefanov and Tulub 2007). The alternative approach is in considering Mg as a spin trigger, which, depending on the system environment and energy, is able to change the spin activity of ATP and thus to direct its cleavage over different spin-dependent reaction paths (Buchachenko and Kuznetsov 2006; Shien et al. 1999; Endres et al. 2004; Tulub 2006; Stefanov and Tulub 2007), including production of $\bullet NMP^{-}$ ($-$ stands for the negative charge and $\bullet$ for the unpaired electron) ion-radicals (Tulub 2006; Stefanov and Tulub 2007). Additionally, it should be stressed that the natural Mg contains 10% of nuclear active spin, ^{25}Mg, and this spin (5/2), through the hyperfine coupling, can initiate unusual reaction paths (Nakagura and Hayashi 2004).

The paper aims at showing that different types of ATP chelation and cleavage, the ionic or ion-radical, come from singlet (S) and triplet (T) reaction paths. These paths arise from the interaction between the Mg water complex and ATP in water solution, which, combined, imitate the real process in a cell. The unique role of Mg appears in its ability to serve a specific redox circuit, accepting an appropriate amount of electron density from ATP and giving it back in portions, thus producing spin-dependent reaction paths, responsible for creating low-energy (stable) and high-energy (quasistable, and unstable) states. The major stress is on proving that

1. S PESs and T PESs are responsible for directing Mg to the O1–O2 and O2–O3 fragments, respectively.
2. Moving along S and T PESs leave Mg with a different number of closely coordinated water molecules.
3. The ion-radical cleavage of ATP comes from electron spin redistribution between the interacting subsystems in the vicinity of a T–T intersection.
4. Mg nuclear spin, ^{25}Mg, affects the ATP cleavage according to the ion-radical mechanism (Tulub 2006).

Since the construction of PESs of different spin symmetry suggests a computational experiment for large systems, like ours, there is no better way at the moment as to address to the widely tested molecular dynamics density functional MD DFT:B3LYP method, allowing to observe the behavior of S and T PESs in a fixed configurational space.

Model and computations

Cellular media mostly consists of water, in which Mg^{2+} appears in a water coat of octahedral configuration (Fig. 1),

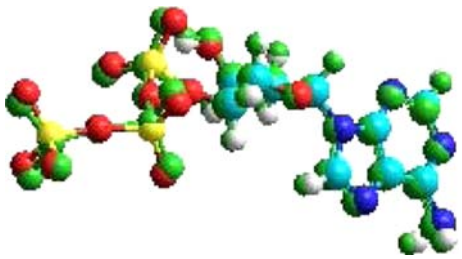

Fig. 2 Imposed structures of ATP in T (multicolored: oxygens – red; phosphorus – yellow; nitrogens – blue; carbons – light blue) and S (monochromic: green) states show slight difference in bond distances and angles

the most stable among other possible configurations (Miessler and Tarr 1991; Misra and Draper 2001; Merrill et al. 2003). With this in mind, it is reasonable to take $Mg[(H_2O)_6]^{2+}$ complex (Mg subsystem) as a realistic Mg cofactor, interacting with ATP (ATP subsystem) in living cell environment (Fig. 1). The geometries of both subsystems were primarily optimized with DFT:B3LYP (6-31G** basis set). The obtained geometry parameters (interatomic distances and angles) for S states are in perfect agreement with the previously obtained ones (Akola and Jones 2003; Merrill et al. 2003; Grigorenko et al. 2006). T states deserve separate consideration.

ATP in T and S states (computations are carried out in the water pool of 78 water molecules with the full geometry optimization, DFT:B3LYP and MDDFT:B3LYP computations, 6-31G** basis set) reveal practically the same value of total energy E^{tot} at $T = 0$ K $E^{tot}(T) < E^{tot}(S)$ by 0.57 kcal/mol that is of a kT level (DFT:B3LYP), and at $T = 310$ K (MD DFT:B3LYP) the barrier is easily overcome, so that both states are entangled over time (Stefanov and Tulub 2007). Figure 2 displays the imposed structures of ATP in T and S states at a frozen point, $T = 0$ K. The deviation in the bond length for both structures does not exceed 0.05 Å. The bond and dihedral angles slightly differ, revealing the most pronounced deviation for the terminal phosphates: in T state the terminal phosphate is turned in the clockwise direction by 36° compared to that of S state, for details see (Stefanov and Tulub 2007). $Mg[(H_2O)_6]^{2+}$ in T state is unstable, the gap in the total energy of T and S states is remarkable, $\Delta E^{tot}(T–S) = 8.3$ eV, (Sanekata et al. 1995; Watanabe et al. 1995; Tulub and Yakovlev 2002; Merrill et al. 2003), and the complex shows tendency to eliminate one hydrogen, finally arising in the form of $[Mg(H_2O)_5OH]^+$ (S or T) with the distorted geometry compared to that of the initial state (Tulub and Yakovlev 2002). With this in mind, in our computations we started from the $Mg[(H_2O)_6]^{2+}$ in its stable S state, which then was converted into the lowest in energy T state via the Franck–Condon excitation in the presence of ATP and water environment, where the gap between the T and S states is much smaller (less than 0.40 eV) than in the case of isolated $Mg[(H_2O)_6]^{2+}$; this leaves the water molecules in the Mg shell undestroyed, see below.

Mg (S state) and ATP (S or T state, see above) subsystems are placed in the water pool of 78 water molecules, surrounding them and meeting the following limits: $R_{OO} \leq 3.60$ Å; $R_{OH} \leq 2.45$ Å; $\phi_{OHO} \leq 45°$ (R_{OO} is the distance between oxygens, R_{OH} is the distance between the oxygen and hydrogen, and ϕ_{OHO} is the angle between two bonds, formed by a hydrogen atom and two oxygen atoms).

The computations are carried out separately for S and T states with the modified MD DFT:B3LYP code NwChem 3.5 plus (NwChem 2006), 6-31G** basis set, installed on a Compaq Alpha Workstation cluster, at a constant human body temperature, $T = 310$ K. Heating to the final temperature, the initial one is 0 K, suggested a step-by-step procedure, each step of 10 K per 1 ps. Subsequent cooling to 0 K occurred in the reverse sequence with the same step. Such a procedure at each step provides reaching thermodynamic equilibrium between Mg and ATP subsystems and the water pool. To obtain reliable statistics, the computations included 750 independent runs ($T = 310$ K), started from randomly initiated points within the area, limited by two distance vectors r[Mg–O2] = 8.0–2.0 Å and r[O2–O1(O3)] = ±4.0 Å (O2 is used as a reference point) and the third one, orthogonal to them (±1 Å). The mutual approaching of the Mg and ATP subsystems in the configuration space, built up on these three vectors, evolved at a step of 0.05 Å (near the crossings the step was reduced to 0.01 Å). The data were subsequently processed with the root-mean-square technique of the Statistica-7.1-Release software (Statistica-7.1 2007). Additionally, around the T–T crossing we used the same computations with switched on hyperfine coupling Hamiltonian, $S_N(^{25}Mg = 5/2)–S_e$. Charges on atoms are computed according to Löwdin's population analysis (Löwdin 1970).

Results and discussion

Initially separated by 8.0 Å (see "Model and computations"), the Mg and ATP subsystems in the pool of 78 water molecules immediately begin to interact by approaching each other and moving along S or T PESs, depending on the spin state of the system. Figure 3a displays S and T PES projection profiles on the imaginary line, connecting the O1, O2, and O3; Fig. 3b is the 3D topside view of these PESs in the configuration space, restricted by r[Mg–(O1–O2–O3)] and the O1–O2–O3 coordinates. At r[Mg–O2] = 8.0 Å the energy gap between the T_2 and S_1 states is 9.8 kcal/mol and between the T_1 and S_1 is 7.4 kcal/mol. Within all the space, the T PESs go above the S ones; in addition, T and S states are remarkably separated in space. The S_1 PES reveals the global

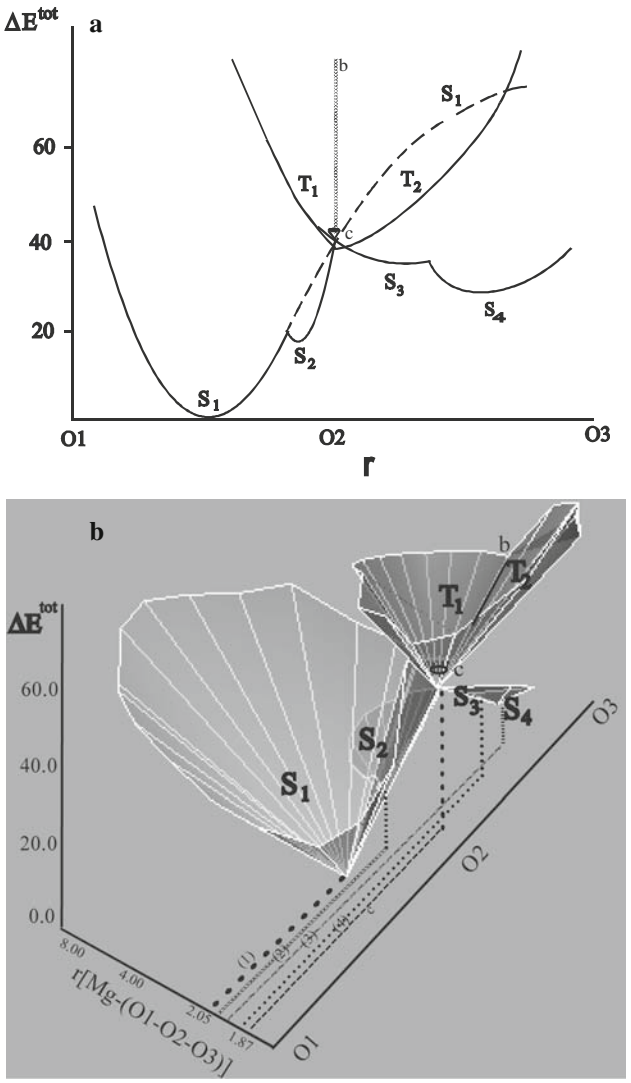

Fig. 3 **a** S and T PES projection profiles on the imaginary line, connecting the O1, O2, and O3 oxygens of ATP. *Solid lines* indicate the front PES profiles and *dashed line* the remote one, **b** corresponds to the barrier, separating T_1 and T_2 PESs, the cone, **c** corresponds to the formation of a spin-separated, ion-radical, state. S_2 and S_3 states are considered as quasi-stable, see text. **b** 3D topside view of S and T PESs in the configuration space, restricted by *r*[Mg–(O1–O2–O3)] and the O1–O2–O3 coordinates; designations correspond to those in Fig. 3a. The values of *r*[Mg–(O1–O2–O3)] are as follows: (1) −2.05 Å, (2) −2.03 Å, (3) −1.95 Å, (4) −2.07 Å, (c) −1.87 Å

minimum (in our computations it is taken as a zero point, $\Delta E^{tot} = 0.0$ kcal/mol), corresponding to the formation of a stable chelate, $[Mg(H_2O)_4{-}(O1{-}O2)ATP]^{2-}$. The distances Mg–O1 and Mg–O2 are identical, *r*[Mg–O1] = *r*[Mg–O2] = 2.05 Å (Table 1). The S_2 has a local minimum, which is by 21.2 kcal/mol higher than that of the global one. The S_2 and S_1 are separated by a low energy barrier of 1.8 kcal/mol, which allows us to consider the S_2 minimum as a metastable, easily surmountable in real cellular environment. The T_1 and T_2 PESs, initially separated by a long-range barrier of 2.7–2.4 kcal/mol, perpendicular to the O1–O2–O3 line and strictly positioned against the O2 atom (*r*[Mg–O2] = 8.0–1.90 Å), exhibit the crossing at *r*[Mg–O2] = 1.90 Å, $\Delta E^{tot} = 39.6$ kcal/mol. This crossing is responsible for producing the S_2, S_3 states and a spin-separated state, see below. The S_3 state reveals a local minimum at $\Delta E^{tot} = 37.8$ kcal/mol, which then transforms into a more stable S_4 state, $\Delta E^{tot} = 34.2$ kcal/mol, the $[Mg(H_2O)_2{}^{-}O2(O3)ATP]^{2-} \Rightarrow [Mg(H_2O)_4{}^{-}O2(O3)ATP]^{2-}$ transition. The spin-separated state, unstable and corresponding to the electron localization on the Mg and ATP subsystems, arises as a small reverse cone (*r*[Mg–O2] = 1.87 Å) of 2.8 kcal/mol height above the T_1–T_2 crossing, Table 1.

The scenario, whereby T and S PESs manifest themselves in the $\Delta E^{tot}{-}r$[Mg–(O1–O2–O3)]−(O1–O2–O3) configuration space, is as follows. Initially, when the interaction between the ATP and Mg subsystems is switched off, the subsystems carry the charge of −4 and +2, respectively. When the interaction is switched on, we observe an immediate charge transfer from the ATP to Mg subsystem, *r*[Mg–(O1–O2–O3)] = 8.0 Å, that results in decreasing the positive charge on the Mg atom from +1.44 to +0.36 (S) and +0.21 (T) and making the original six-coordinated Mg water complexes unstable. Slightly charged, the Mg complexes in S and T states begin to lose a part of their initially coordinated water molecules. The loss of water molecules is not stochastic and suggests that the two remotest from the ATP water molecules (H_2O^5 and H_2O^4, Mg subsystem Fig. 1) begin to leave the original complex one by one. This is accompanied by changing the interatomic distances and angles within each complex, but these changes are not dramatic. When the distance r[Mg-$O^5(O^4)H_2$] reaches the values of 2.60(S)–2.75(T), one can observe a regrouping between the rest water molecules in such a way that opens direct Coulomb interactions between the Mg and the O1, O2, and O3 atoms (H_2O^6, H_2O^1, H_2O^2, and H_2O^3 appear to be turned away from the O1–O2–O3 line), Fig. 1. Up to this moment, the picture is practically identical to S and T states, *r*[Mg–(O1–O2–O3)] = 7.55(S)–7.50(T) Å, so that the changes mostly affect the Mg subsystem leaving the ATP one practically undisturbed. This is in agreement with the previous results showing that the isolated ATP in S and T states has the same energy.

After the regrouping (H_2O^5 and H_2O^4 are removed from the complex by 3.7 (S) and 4.2 (T) Å, respectively), the positive charge on Mg begins to restore, but the rate and extent of this process for T and S states are different (Fig. 4). The S state gains the positive charge faster than the T one. This, in turn, produces differences in a further evolution of the system. In S state the Mg, with its higher positive charge, retains four water molecules in its coordination shell and experiences the Coulomb attraction to

Table 1 Mg–ATP complexes of different spin and energy, ΔE^{tot} (kcal/mol)

Complex	Spin state	ΔE^{tot}	r(Mg-O1)	r(Mg-O2)	r(Mg-O3)
$[Mg(H_2O)_2-(O2)\{O1\}ATP]$	T_1 (unstable)	≥39.6		≥1.90	
$[Mg(H_2O)_2-(O2)\{O3\}ATP]$	T_2 (unstable)	≥39.6		≥1.90	
$[Mg(H_2O)_2-(O2\text{-}O3)ATP]$	S_3 (metastable)	37.8		1.95	2.04
$[Mg(H_2O)_4-(O2\text{-}O3)ATP]$	S_4 (stable)	34.2		2.07	2.07
$[Mg(H_2O)_3-(O2)\{O1\}ATP]$	S_2 (metastable)	21.2		2.02	2.46
$[Mg(H_2O)_4-(O2\text{-}O1)ATP]$	S_1 (stable)	0.0	2.05	2.05	
$[\bullet Mg(H_2O)_2-\bullet(O2)ATP]$	c (unstable)	42.4		1.87	

With reference to Mg–O (1, 2, 3) distances, Å; in { } are the oxygens remote from the Mg

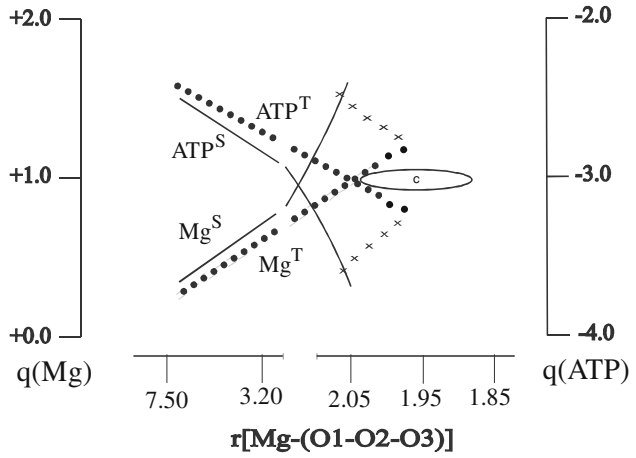

Fig. 4 Change in Mg and ATP charge (q) as a function of the Mg–(O1–O2–O3) distance. *Solid lines* correspond to S states and *dotted lines* to T states; ellipse (c) indicates the area of a spin-separated state, $[\bullet Mg^{+}(H_2O)_2-\bullet(O2)ATP^{-3}]$; curves marked with *crosses* indicate charge reduction over transition from $[Mg(H_2O)_2-(O2,\{O3\})ATP]$ to $[Mg(H_2O)_4-(O2-O3)ATP]$, see text

the O1–O2 fragment, bypassing a close approach to the O2 atom, $r[Mg\rightarrow O2] \geq 2.80$ Å (the arrow indicates the direction of the virtual single-bond formation). This comes from the fact that the O1–O2 fragment carries a higher negative charge than the O2–O3 one: q(O1) = −0.94, q(O2) = −0.87, q(O3) = −0.82. Approaching between the $Mg(H_2O)_4$ and ATP subsystems along the S_1 PES (r[Mg–(O1–O2) = 7.50–2.05 Å] finally results in forming a stable chelate, $[Mg(H_2O)_4-(O1-O2)ATP]$, of S symmetry (Fig. 3a, b). The intermediate product with a singly charged Mg^{+} and ATP^{3-}, $[Mg^{+}(H_2O)_4-ATP^{3-}]^{S}$ (r[Mg–(O1–O2–O3)] = 2.80 Å), reveals no spin localization on the Mg and ATP subsystems unlike that of T state, $[Mg^{+}(H_2O)_2-ATP^{3-}]^{T}$, see below.

In T state the Mg carries a lower positive charge, and the ATP terminal phosphate, $P_\gamma O_3$, appears to be slightly removed from the rest part of ATP ($r[P_\gamma–O_\gamma]$ is increased by 0.17 Å compared to that of the isolated ATP (Stefanov and Tulub 2007))—a result of ATP perturbation from the Mg subsystem, when the two subsystems experience the Coulomb approach, r[Mg–(O1–O2–O3)] ≤ 7.50–1.90 Å. This makes the O1–O2 fragment be lower charged compared to that of the O2–O3 one [q(O1) = −0.52, q(O2) = −0.89, q(O3) = −0.68] and makes $[Mg(H_2O)_4]^{T}$ move initially towards the O2 atom. On its way along the T_1 or T_2 PESs, $[Mg(H_2O)_4]^{T}$ loses consecutively two additional water molecules in the distance interval r[Mg–(O2)] = 7.50–2.20 Å (H_2O^3 and H_2O^6 appear to be separated from the Mg by 2.78 and 2.83 Å, respectively) and converts into $[Mg(H_2O)_2]^{T}$.

The crossing between the T_1 and T_2 PESs *r[Mg–O2] = 1.90 Å, ΔE^{tot} = 39.6 kcal/mol, deserves a separate discussion because it generates a number of states, differing in spins. The T_1 and T_2 come to the crossing having their total spins oriented in parallel, Fig. 5 (right). This is the evidence from the spin density analysis and the fact that the T_1 and T_2 PESs in the region r[Mg–(O1–O2–O3)] ≥ 1.90 Å are separated by the energy barrier, see above. The crossing state is unstable and implies transformation into two quasistable S states (S_2 and S_3), Fig. 5 (left), and a spin-separated state, showing the oppositely oriented spin localization on the $Mg^{+}(H_2O)_2$ and ATP^{-3} within the intermediate $[\bullet Mg^{+}(H_2O)_2-\bullet(O2)ATP^{-3}]$ (ΔE^{tot} = 42.4 kcal/mol), Fig. 5 (top left), Fig. 3a, b, Table 1.

The S_2 and S_3 states reveal the local minima, which could be assigned, respectively, to the appearance of $[Mg(H_2O)_3-(O2,\{O1\})ATP]$ (ΔE^{tot} = 21.2 kcal/mol; q[Mg] = +1.38)

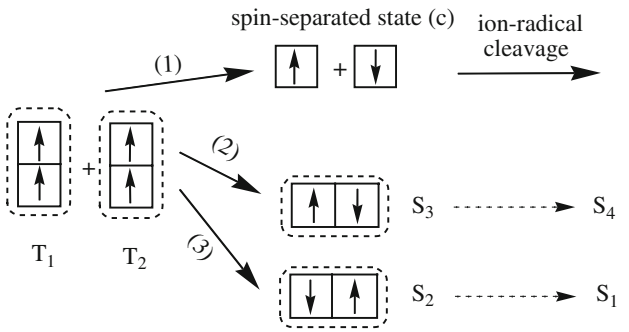

Fig. 5 Spin states appearing upon interaction of T_1 and T_2 PESs around the crossing. *(1)* corresponds to the production of a spin-separated state followed by ATP cleavage according to ion-radical mechanism, *(2)* and *(3)* correspond to the production of metastable S_3 and S_2 states suggesting their further transformations into S_4 and S_1

and $[Mg(H_2O)_2–(O2–O3)ATP]$ ($\Delta E^{tot} = 37.8$ kcal/mol; $q[Mg] = +1.22$) complexes, Table 1 (in { } are the oxygens, which are remote from the Mg). The major difference in these complexes is that moving along the S_2 PES the $Mg(H_2O)_2$ adds the third water molecule and turns into a four-coordinated complex (the O1 atom is distanced from the Mg by 2.46 Å and affects the complex at a perturbation level), more stable than a three-coordinated one (Merrill et al. 2003). The S_3 state gains a four-coordinated stabilization by making a chelate $[Mg(H_2O)_2–(O2–O3)ATP]$ ($r[Mg–O2] = 1.95$ Å; $r[Mg–O3] = 2.04$ Å).

The S_2 and S_3 states suggest their further transformations into more stable six-coordinated complexes: this occurs through adding (S_2) the fourth water molecule ($r[Mg–OH_2] = 2.14$ Å) and forming a stable chelate, $[Mg(H_2O)_4–(O1-O2)ATP]$ (the S_1 state; $q[Mg] = 1.74$; $r[Mg–O1] = r[Mg–O2] = 2.05$ Å) (Table 1, Fig. 3a, b). In case of the S_3 state, the stabilization occurs through adding two water molecules with the distances $r(Mg–OH_2) = 2.16$ and 2.23 Å. The appeared chelate $[Mg(H_2O)_4–(O1–O3)ATP]$ (S_4 state; $q[Mg] = 1.66$) has the identical distances $r[Mg–O2] = r[Mg–O3] = 2.07$ Å. The $S_2 \rightarrow S_1$ and $S_3 \rightarrow S_4$ transitions suggest overcoming small energy barriers of 1.8 and 1.4 kcal/mol, respectively.

The spin-separated intermediate $[\bullet Mg^+(H_2O)_2–\bullet(O2)ATP^{-3}]$ is highly unstable and undergoes a rapid decomposition according to the ion-radical mechanism (1) (Tulub 2006; Stefanov and Tulub 2007):

$$\left[\bullet Mg^+(H_2O)_2 - \bullet(O2)ATP^{3-}\right] \xrightarrow{(1)} PO_3^- + \left[\bullet Mg^+(H_2O)_2 - \bullet(O2)ADP^{2-}\right] \xrightarrow[H_5O_2^+]{(2)} HP_2O_7^{2-} + [Mg(H_2O)_4]^{2+} + \bullet AMP^- \quad (1)$$

Reaction (1) consists of two steps: first, production of the adenosinediphosphate ion-radical, $\bullet ADP^{2-}$, (1), bound to the $\bullet Mg^+(H_2O)_2$ within the complex $[\bullet Mg^+(H_2O)_2–\bullet(O2)ADP^{-3}]$, and, second, production of the adenosinemonophosphate ion-radical, $\bullet AMP^-$, (2) upon interaction with the Zundel cation, $H_5O_2^+$ (Zundel 2000), acidic media.

The hyperfine interaction included, the barrier, initially separating the $T_1–T_2$ crossing and the spin-separated state (c), vanishes ($\Delta E^{tot}[T_1–T_2] = 39.1$ kcal/mol; $r[Mg–O2] = 1.87$ Å). This results in the domination of the (c) state over the others: ΔE^{tot} (c) = 38.5 kcal/mol; ΔE^{tot} (S_3) = 40.4 kcal/mol; $\Delta E^{tot}(S_2) = 39.8$ kcal/mol. The finding supports the idea that the active Mg nuclear spin, ^{25}Mg, can affect the ATP cleavage according to the ion-radical mechanism (Stefanov and Tulub 2007). Seemingly, 10% content of ^{25}Mg in natural Mg is responsible for this effect.

Concluding remarks

The computations show that ATP can realize different in energy states thanks to its interaction with the Mg water complexes, whose spin state, S or T, dictates the way of binding. The role of Mg appears in its redox activity: initially, Mg accepts the electron density from ATP and then donates it back in portions, depending on the system's spin state. This donation affects the number of bound water molecules and thus regulates the ATP energetics. Strong chelation, accompanied by producing S states, favours the formation of stable Mg–ATP complexes, whereas single-bonded complexes are unstable because the odd number (n) of ligands, bound to Mg within its first coordination shell, generally introduces instability into the Mg subsystem (Pavlenko and Voityuk 1991). This is particularly true for $n = 3$ like in the case of the $[Mg(H_2O)_2–(O2)ATP]$ complex.

Different energy states affect the activity of Mg–ATP complex. The S_1 state is the most stable. The experiment reveals that Mg preferably binds to the O1–O2 fragment. The S_4 state is distinguished by a higher energy from that of the S_1 and seems less preferable for chelating by Mg (Williams 2000). Considering that conventional hydrolysis follows the ionic reaction mechanism (Akola and Jones 2003; Grigorenko et al. 2006), one can believe that ATP cleavage requires a different starting energy for S_1 and S_4 states (this comes from the fact that the energy barriers differ by three times, Table 1). This, in turn, suggests that Mg complexation to the O2–O3 fragment leads to significant rate enhancement, experimentally observed by Williams (Williams 2000).

The spin-separated state, owing to the formation of a highly unstable complex $[\bullet Mg(H_2O)_2–\bullet(O2)ATP]$, initiates the earlier unknown ion-radical reaction path, proceeding at a rate, which is around ten orders faster than the conventional hydrolysis [reaction (1)]. (Tulub 2006; Stefanov and Tulub 2007). This was earlier proved with the CIDNP technique on ^{31}P nuclei, allowing to detecting short-living free radical pairs. The experiment (Tulub 2006) involved a Mg-dependent GTP assembly in a glucose with a dissolved $MgCl_2$ salt on a Mg-dependent DNA-I polymerase support, which provides blocking of O1, O4 and O5 (Fig. 1). After a 75 fs laser impulse, obtained from a Ti–sapphire self-adjusting laser, the assembly, showing a lag of 10^2–10^3 ps, started. The CIDNP polarization spectra, displaying slow intensity decay over a period of 10^4 μs, revealed oppositely polarized absorbances at 6.8 and −10.2 ppm, which could be assigned to $HP_2O_7^{3-}$ and $\bullet GMP^-$, respectively. Without Mg, the CIDNP experiment reveals no polarization spectra. The latter is highly intriguing with regard to reaction (1) and the role of Mg in producing local magnetic fields affecting the rate and path of biochemical reactions.

One can confidently suggest that in cell solution Mg appears as a typical spin catalyst. Our computational experiment, which is initially restricted to the accepted model (see above), predicts a relatively low amount of energy to convert the Mg complex from its ground S state to the nearest T one. In real cellular environment, the gap between S and T states could be significantly lower and controlled by some weakly-bound to the Mg complex biological aggregates (BAs) like DNA polymerases, see above. Depending on the BA function and the environment, the Mg complex appears in S or T state, thus initiating NTP cleavage according to the ionic or ion-radical path. These effects are highly local and hardly affected by external magnetic fields, even strong enough, due to screening Mg–ATP complexes by thick layers of water and proteins. However, with a short-time femtosecond/achtosecond laser excitation, tuned on a particular S→T transition in the Mg complex in its natural/water environment, we can directly manipulate the rate and path of NTP cleavage. This seems to be of importance to nanotechnologies and biocomputing.

The fact that ^{25}Mg can facilitate the ATP cleavage (this comes from decreasing the energy barrier, see above) makes one think that Mg has been chosen by nature as a major ATP cofactor not randomly. The natural Mg has a relatively low content of nuclear active spin (but seems quite enough for initiating ion-radical reactions in living cells), which, in turn, reveals the lowest spin excitation energy among other possible candidates. Zn, for instance, is the closest element to Mg by its nuclear spin properties, but unlike Mg it fails to support the appropriate redox conversion (Tulub 2002). In conclusion, we really do believe that the active nuclear spin of Mg is responsible for initiating the ion-radical cleavage of NTP (not published experimental results), and thus for multiple assembly processes (tubulin assembly, e.g.) accompanied by this cleavage in living nature; this is true provided that the Mg complex is in its T state.

Acknowledgments The research is supported by the Ministry of Education of Russian Federation (Grant RNP 2.1.1.4139) and NASA Ecology Program for providing access to necessary computer resources.

References

Akola J, Jones R (2003) ATP hydrolysis in water—a density functional study. J Phys Chem B 107:11774–11783

Audesirk T, Audesirk G (1999) Biology, life on earth. 5th edn. Prentice-Hall, London

Boyer P (1997) Energy, life, and ATP. Nobel Prize Lecture Elsevier Publ. Comp, Amsterdam

Buchachenko A, Kuznetsov D (2006) Magnesium isotopic effect: a key towards mechanochemistry of phosphorylating enzymes as molecular machines. Russ Mol Biol 40:12–19

Endres R, Cox D, Singh R (2004) The quest to high-conductance DNA. Rev Mod Phys 76:195–214

Grigorenko B, Rogov A, Nemukhin A (2006) Mechanism of triphosphate hydrolysis in aqueous solution: QM/MM simulation in water clusters. J Phys Chem B 110:4407–4412

Dustin P (1984) Microtubules. 2nd edn. Springer, Berlin

Korolev G, Marchenko A (2000) Living chain radical polymerization. Russ Adv Chem 69:447–475

Levy C (1982) Elements of biology. Addison–Wesley, New York

Löwdin P (1970) On the nonorthogonality problem. Adv Quant Chem 5:185–199

Merrill G, Webb S, Bivin D (2003) The formation of alkali metal/alkaline earth cation water clusters, $M(H_2O)_{1-6}$, $M = Li^+$, Na^+, K^+, Mg^{2+}, and Ca^{2+}: an effective fragment potential (EFP) case study. J Phys Chem A 107:386–396

Miessler G, Tarr D (1991) Inorganic chemistry. Prentice-Hall, Princeton

Minehardt T, Marzari N, Cooke R, Pate E, Kollman P, Car R (2002) A classical and Ab initio study of the interaction of the myosin triphosphate binding domain with ATP. Biophys J 82: 660–675

Misra V, Draper D (2001) A thermodynamic framework for Mg^{2+} binding to RNA. Proc Natl Acad Sci USA 98:12456–12461

Nakagura S, Hayashi H (2004) Dynamic spin chemistry: magnetic controls and spin dynamics of chemical reactions. Wiley, New York

Nave C, Nave B (1985) Physics for the health sciences. 3rd edn. W Saunders, New York

Nelson P (2004) Biological physics. WH Freeman, New York

Nelson D, Cox M (2004) Lehninger principles of biochemistry. 4th edn. WH Freeman, New York

NwChem (2006) A Computational Chemistry Package for Parallel Computers, Version 3.5 plus, Pacific Northwest Laboratory, Richland

Ochoa S (1964) Enzymatic synthesis of ribonucleic acid. Nobel Prize Lecture. Elsevier Publ. Comp, Amsterdam

Odian G (1991) Principles of polymerization. Wiley, Canada

Okimoto N, Yamanaka K, Ueno J, Hata M, Hoshino T, Tsuda M (2001) Theoretical studies of the ATP hydrolysis mechanism of myosin. Biophys J 81:2786–2794

Pavlenko S, Voityuk A (1991) Structure and energetics of water magnesium complexes. Russ J Struct Chem 32:155–158

Sanekata M, Misaizu F, Fuke K, Iwata S, Hashimoto K (1995) Reactions of singly charged alkaline-earth metal ions with water clusters: characteristic size distribution of product ions. J Am Chem Soc 117:747–754

Sept D, Limbach H-J, Bolterauer H, Tuszynski JA (1999) A chemical kinetics model for microtubule oscillations. J Theor Biol 197:77–88

Shien Z, Luo T, Hwang L (1999) Mg NMR relaxation study of Mg-ATP complexation in solution. J Chin Chem Soc 46:759–772

Statistica –7.1 Release (2007) Stat. Package. StatSoft Ltd., Tulsa, USA

Stefanov V, Tulub A (2007) Ion-radical mechanism of nucleosidet-riphosphate cleavage to nucleosidemonophosphate upon interaction with mg^{2+} and the radical nature of single DNA chain synthesis. Doklady Akademii Nauk of the Russian Federation, Ser. Biochem Biophys Mol Biol 414:313–316

Stryer L (2002) Biochemistry. 4th edn. W Freeman, New York

Tulub A (2002) The Grignard reaction is a result of tunneling the triplet reaction path through the singlet barrier. J Obschei Khimii (J General Chemistry) 76:948–955

Tulub A (2004) DFT:B3LYP ab initio Molecular Dynamics Study of the Zundel and Eigen Protons complexes in the Triplet State in Gas Phase and Solution. 120:1217–1222

Tulub A (2006) Molecular dynamics DFT:B3LYP study of guanosinetriphosphate conversion into guanosinediphosphate upon

Mg^{2+} chelation of alpha and beta phosphate oxygens of the triphosphate tail. Phys Chem Chem Phys 8:2187–2192

Tulub A (2006) Ion-radical versus hydrolytic mechanism of adenosine/guanosine triphosphate cleavage. Phys Chem Chem Phys 8:5368–5369

Tulub A, Yakovlev D (2002) Restructuring of $[M(H_2O)_6]^{2+}$ (M = Mg,Ca) solvation shell in hydrogen elimination and electron capture in triplet and singlet states. Russ J Phys Chem 76:455–458

Tulub A, Stefanov V (2004) Activaton of tubulin assembly into microtubules upon a series of repeated femtosecond laser impulses. J Chem Phys 121:11345–11350

Tuszynski J, Dixon J (2002) Biomedical applications of introductory physics. Wiley, London

Walker J (1997) ATP synthesis by rotary catalysis. Nobel prize lecture. Elsevier, Amsterdam

Watanabe H, Iwata S, Hashimoto K, Misaizu F, Fuke K (1995) Molecular orbital studies of the structure and reactions of singly charged magnesium ion with water clusters, $Mg^{+}(H_2O)_n$. J Am Chem Soc 117:755–763

Williams N (2000) Magnesium ion catalyzed ATP hydrolysis. J Am Chem Soc 122:12023–12024

Zundel G (2000) Hydrogen bonds with large proton polarizabilities and proton transfer processes in electrochemistry and biology. Adv Chem Phys 111:1–217